Epigenetic heterogeneity of the Notch signaling components in the developing human retina

Takahiro Nakayama[1], Masaharu Yoshihara[2], Satoru Takahashi[3,4]

[1] College of Medicine, School of Medicine and Health Sciences, University of Tsukuba
[2] Department of Primary Care and Medical Education, Institute of Medicine, University of Tsukuba
[3] Department of Anatomy and Embryology, Institute of Medicine, University of Tsukuba
[4] Transborder Medical Research Center, Institute of Medicine, University of Tsukuba

Article type
Article

Corresponding author
Masaharu Yoshihara, MD, PhD
Assistant Professor
Institute of Medicine, University of Tsukuba
(Postal code) 1-1-1 Tennodai, Tsukuba, Ibaraki, 305-8575, Japan
(Phone) 81-29-853-7516
(FAX) 81-29-853-6965
(E-mail) yoshihara.masahar.ly@alumni.tsukuba.ac.jp

E-mail addresses
Takahiro Nakayama: nakayama.takahiro.rp@alumni.tsukuba.ac.jp
Masaharu Yoshihara: yoshihara.masahar.ly@alumni.tsukuba.ac.jp
Satoru Takahashi: satoruta@md.tsukuba.ac.jp

ORCID IDs
Takahiro Nakayama: 0000-0002-4023-4560
Masaharu Yoshihara: 0000-0002-0212-0909
Satoru Takahashi: 0000-0002-8540-7760

Abstract
Notch signaling-mediated differentiation is dependent on fine-tuned expression regulation. In particular, the diversification processes of the initially homogenous undifferentiated cells

were well documented for this signaling pathway. Although this signaling pathway is involved in the development of the mammalian retina, it is unclear how the expression levels of Notch signaling components are regulated. Here, we analyzed publicly available datasets of single-cell RNA-seq and single-cell ATAC-seq from human fetal retinas at Days 53, 59 and 78 to examine the status of the mRNA expression and chromatin accessibility of Notch signaling components. We found that Notch signaling components were expressed in undifferentiated cells and that the chromatin accessibilities in those cells were different. This finding revealed the epigenetic heterogeneity among the differentiating cells during Notch signaling-driven cellular dynamics.

Introduction

The Notch signaling pathway is essential for the development of the nervous system, including the retina (1). Indeed, a transgenic mouse study revealed that most retinal cells received Notch1 signaling (2). Along with inducing differentiation, this signaling pathway is known to generate the fine-grained cell arrangement of differentiated cells from initial undifferentiated cells in *Drosophila* neurogenesis (3). Lateral inhibition with a feedback mechanism that is supported by the low surface expression rate of DSL ligands in NOTCH signaling-receiving cells has been well documented to generate this fine-grained pattern (4). Indeed, the oscillation of Dll1 (one of the mammalian DSL ligands) mRNA levels is critical in somitogenesis (5). Another computer simulation study suggested that the redundant expression of both DSL ligands and NOTCH receptors was essential for the generation of fine-grained patterns via ligand receptor interactions (6). Importantly, initial homogeneity is assumed in previous computer simulation studies (4) (6) (7).

Single-cell multiomics has enabled genome-wide examination of mRNA expression (8) and chromatin accessibilities (9). Combining single-cell RNA-seq (scRNAseq) and single-cell ATAC-seq (scATACseq) reveals chromatin accessibilities of genes of interest in a specific cell population. For example, the retina is composed of three neuron layers (photoreceptor, bipolar cell, and retinal ganglion cell layers) intercalated with amacrine cells and horizontal cells. Since these differentiated cells arise from a single progenitor cell (multipotent progenitor cells, MPCs), it is important to distinguish the specific cell stages where Notch signaling is active. Since the scRNA-seq and scATAC-seq datasets from human fetal retinas (Days 53, 59 and 78) were recently reported (10), in this study, the chromatin accessibilities in the differentiating cells were analyzed to examine the homogeneity in the Notch signaling components from an epigenetic perspective.

Results

scRNA-seq and scATAC-seq analysis of Day 53 fetal retina

We started with the dataset from the youngest fetus (Day 53, d53). We carried out principal component analysis (PCA) followed by uniform manifold approximation and projection (UMAP), which generated seven clusters (Figure 1A). Unfortunately, two clusters were characterized by mitochondrial genes, suggesting that these cell populations represented dead cells (dead1 and dead2). The remaining cells were largely undifferentiated cells that were characterized with CCND1 (MPC marker) (11) or PLXNA2 (retinal progenitor cell marker, RPC) (12) (Figure 1B). One small cluster was characterized by POU4F2 (retinal ganglion cell marker, RGC) (11). In mammals, this signaling pathway consists of five DSL ligands (JAG1, JAG2, DLL1, DLL3 and DLL4), four NOTCH receptors (NOTCH 1-4) and several downstream target genes, such as HES1, HES5, HEY1 and HEY2 (13). JAG1 and DLL1 were expressed in MPCs (Figure 1C), while NOTCH1, NOTCH2 and NOTCH3 were expressed in MPCs (Figure 1D). As expected, HES1 was expressed in MPCs (Figure 1E). Next, we analyzed the scATAC-seq dataset from the same d53 fetus using the ArchR package (21). We took an iterative latent semantic indexing (Iterative LSI)-based method for UMAP-based clustering that generated nine clusters. Since the scRNAseq analysis suggested NOTCH receptor expression in the CCND1-expressing undifferentiated cells, we examined chromatin accessibilities near the CCND1-coding site (100 kb on either side of the gene). The violin plot showed that the two clusters had high gene scores (C3 and C4; arrowheads) (Figure 1G). One of these clusters (C3) also had a high gene score for JAG1, while the other (C4) had a low gene score owing to a zero score in more than 25% of these cells (Figure 1H). Concerning the downstream target gene HES1, both the C3 and C4 clusters had high gene scores (Figure 1I). In summary, we observed heterogeneity in chromatin accessibility near JAG1 among undifferentiated cell populations (C3 and C4). The violin plots for the other Notch signaling components are available in Supplementary Fig. S1. For example, concerning DLL1 and NOTCH1, both C3 and C4 had high gene scores. By contrast, C3 and C4 had high gene scores for NOTCH3 and HES5, respectively. To our surprise, the gene scores for NOTCH2 were low in C3 and C4.

scRNA-seq and scATAC-seq analysis of Day 59 fetal retinas

Then, we analyzed the dataset from the Day 59 fetus (d59). PCA followed by UMAP clustering generated six clusters (Figure 2A). We used ELAVL4 (14) and PLXNA2 (12). CPLX2 (15) and OTX2 (16) are markers of RGCs, RPCs, differentiating amacrine cells (dAMA) and the common progenitor cells for cones/rods (CON/ROD), respectively (Figure 2B). The dAMA cluster coexpressed DSL ligands (DLL 1-3), NOTCH1 and downstream target genes (HES5 and HEY1) (Figure 2C-2E). The iterative LSI-based method for

UMAP-based clustering generated fifteen clusters. The clusters 1-8, 11, 13 had high gene scores for CPLX2. Among these, only C7 and C13 had high gene scores for DLL4 (Figure 2H). In addition, the gene score for HES5 were enriched only in C13 among the clusters 1-8, 11, 13 (Figure 2I). These observations suggested that dAMA cells were epigenetically heterogenous in the DLL4 chromatin accessibility and HES5 responsiveness. The violin plots for the other Notch signaling components are available in Supplementary Fig. S2.

scRNA-seq and scATAC-seq analysis of Day 78 fetal retina

Finally, we analyzed the dataset from the Day 78 fetus (d78). PCA followed by UMAP clustering generated nine clusters (Figure 3A). We used MYBL1 (17) as a marker of RPC in addition to the other markers (CCND1, OTX2, ELAVL4 and PLXNA2) (Figure 3B). MPC1 were rich in the expression of NOTCH1, HES1 and HES5, whereas RPC3 were rich in the expression of DLL1, DLL4, NOTCH1 and HES5 (Figure 3C-3E). The iterative LSI-based method for UMAP-based clustering generated ten clusters where only C6 (arrowheads) had high gene scores for CCND1, NOTCH1 and HES1 (Figure 3G-3I). The concomitant high gene scores for NOTCH1 and HES5 in C6 were reasonable because many cells had undergone differentiation at this developmental stage. Therefore, it was difficult to identify the heterogeneity in the Notch signaling components that was observed in d53 and d59. The violin plots for the other Notch signaling components are available in Supplementary Fig. S3. Unfortunately, RPC3 cell population was unidentifiable in this scATAC-seq analysis owing to low gene scores for MYBL1.

Discussion

Patterning morphogenesis via the Notch signaling pathway has been studied for decades and is thought to be mediated by fine-tuned regulation of the surface expression of Notch signaling components. For example, Mindbomb (MIB) increases the surface trafficking of DLS ligand proteins via ubiquitination (18). The underlying molecular mechanism, however, is still unclear at a transcription regulation level. Recently, an upstream epigenetic regulator, Stuxnet (stx), was reported to promote Notch receptor mRNA expression in *Drosophila* (19). It is, however, less documented whether there is epigenetic heterogeneity among differentiating cells. In this study, we identified the heterogeneity of Notch signaling components among undifferentiated cells at an epigenetic level that potentially impacts the transcriptional control of Notch signaling components. In addition, while previous computer simulation studies assumed initial homogeneity with fluctuation, this study questioned this assumption. Since our observation might focus on the middle of retinal development, further examination is warranted using samples at earlier developmental stages that are not

currently available. In addition, the impact of this epigenetic heterogeneity on patterning morphogenesis is a target of future studies.

There are several limitations in the present study. First, this study is an observational study from a single sample at each developmental stage (d53, d59 and d78). Therefore, it is necessary to carry out additional sampling or interventional animal experiments to examine the validity of the information reported in this study. Second, the correlations between the mRNA expression in scRNA-seq and the gene scores in scATAC-seq had potential uncertainty owing to different clustering methods between scRNA-seq and scATAC-seq. Third, without further examination, the idea of heterogeneity is not generalizable to other biological contexts where Notch signaling is in action.

Methods

The scRNA-seq and scATAC-seq datasets for the human fetal retinas at Days 53, 59 and 78 were downloaded from Gene Expression Omnibus (https://www.ncbi.nlm.nih.gov/geo/) (Accession Number GSE183684) (10). For the analysis of scRNA datasets, Seurat version 4.3.0.1 (20) was used in R version 4.3.1 (21) under macOS Ventura 13.4.1. Since the dataset d53 contained many dead cells with increased mitochondrial genes, the cells with less than three percent mitochondrial genes were selected for further analysis. After dimension reduction with PCA and clustering with UMAP, 2000 highly variable features across 2111 cells were finally used for the analysis. For datasets d59 and d78, the threshold of the percentage of mitochondrial genes was set to five. The numbers of highly variable genes were set to 2000, and the final cell numbers analyzed were 5755 cells for dataset d59 and 5997 cells for dataset d78.

For the analysis of scATACseq dataset, ArchR (22) was used in R version 4.3.1 (21) under macOS Ventura 13.4.1. For the dataset d53, minimal TSS score was set to zero to collect enough number of the cells for the analysis. The other parameters were set to the default values. The numbers of cells analyzed were 9103, 7249 and 10399 for d53, d59 and d78, respectively. The numbers of median TSS were 9.499, 11.342 and 10.843 for d53, d59 and d78, respectively. The numbers of median Frags were 12522, 13996 and 10192 for d53, d59 and d78, respectively.

References

1. Chen, X. & Emerson, M. M. Notch signaling represses cone photoreceptor formation through the regulation of retinal progenitor cell states. *Sci. Rep.* **11**, 14525; 10.1038/s41598-021-93692-w (2021).
2. Yoshihara, M. *et al*. Generation of a Gal4-dependent gene recombination and

illuminating mouse. *Exp. Anim.* **71**, 385-390 (2022).

3. Heitzler, P. & Simpson, P. The choice of cell fate in the epidermis of Drosophila. *Cell.* **64**, 1083-1092 (1991).
4. Collier, J. R., Monk, N. A., Maini, P. K. & Lewis, J. H. Pattern formation by lateral inhibition with feedback: a mathematical model of delta-notch intercellular signalling. *J. Theor. Biol*. **183**, 429-446 (1996).
5. Shimojo, H. *et al*. Oscillatory control of Delta-like1 in cell interactions regulates dynamic gene expression and tissue morphogenesis. *Genes Dev*. **30**, 102-116 (2016)
6. Yoshihara, M. *et al*. Mathematical analysis of the effect of portal vein cells on biliary epithelial cell differentiation through the Delta-Notch signaling pathway. *BMC Res. Notes*. **14**, 243; 10.1186/s13104-021-05656-y (2021).
7. Sprinzak, D., Lakhanpal, A., LeBon, L., Garcia-Ojalvo, J. & Elowitz, M. B. Mutual inactivation of Notch receptors and ligands facilitates developmental patterning. *PLoS Comput. Biol*. **7**, e1002069; 10.1371/journal.pcbi.1002069 (2011).
8. Tang, F. *et al*. mRNA-Seq whole-transcriptome analysis of a single cell. *Nat. Methods*. **6**, 377-382 (2009).
9. Buenrostro, J. D. *et al*. Single-cell chromatin accessibility reveals principles of regulatory variation. *Nature*. **523**, 486-490 (2015).
10. Lyu, P. *et al*. Gene regulatory networks controlling temporal patterning, neurogenesis, and cell-fate specification in mammalian retina. *Cell Rep*. **37**, 109994; 10.1016/j.celrep.2021.109994 (2021).
11. Finkbeiner, C. *et al*. Single-cell ATAC-seq of fetal human retina and stem-cell-derived retinal organoids shows changing chromatin landscapes during cell fate acquisition. *Cell Rep*. **38**, 110294; 10.1016/j.celrep.2021.110294 (2022).
12. Emerson, S. E. *et al*. Identification of target genes downstream of semaphorin6A/PlexinA2 signaling in zebrafish. *Dev. Dyn*. **246**, 539-549 (2017).
13. Kopan, R. & Ilagan, M. X. The canonical Notch signaling pathway: unfolding the activation mechanism. *Cell*. **137**, 216-233 (2009).
14. Wu, F. *et al*. Single cell transcriptomics reveals lineage trajectory of retinal ganglion cells in wild-type and Atoh7-null retinas. *Nat. Commun*. **12**, 1465; 10.1038/s41467-021-21704-4 (2021).
15. Reim, K. *et al*. Aberrant function and structure of retinal ribbon synapses in the absence of complexin 3 and complexin 4. *J. Cell Sci*. **122**, 1352-1361 (2009).
16. Emerson, M. M., Surzenko, N., Goetz, J. J., Trimarchi, J. & Cepko, C. L. Otx2 and Onecut1 promote the fates of cone photoreceptors and horizontal cells and repress rod photoreceptors. *Dev. Cell*. **26**, 59-72 (2013).

17. Kaufman, M. L. *et al*. Transcriptional profiling of murine retinas undergoing semi-synchronous cone photoreceptor differentiation. *Dev. Biol*. **453**, 155-167 (2019).
18. Scavuzzo, M. A. *et al*. Pancreatic Cell Fate Determination Relies on Notch Ligand Trafficking by NFIA. *Cell Rep*. **25**, 3811-3827.e7; 10.1016/j.celrep.2018.11.078 (2018).
19. He, T. *et al*. Stuxnet fine-tunes Notch dose during development using a functional Polycomb response element. *Development*. **150**, dev201297; 10.1242/dev.201297 (2023).
20. Hao, Y. *et al*. Integrated analysis of multimodal single-cell data. *Cell*. **184**, 3573-3587 (2021).
21. R Core Team (2023). _R: A Language and Environment for Statistical Computing_. R Foundation for Statistical Computing, Vienna, Austria. <https://www.R-project.org/>.
22. Granja, J. M. *et al*. ArchR is a scalable software package for integrative single-cell chromatin accessibility analysis. *Nat. Genet*. **53**, 403-411 (2021).

Acknowledgments

This work was supported by JSPS KAKENHI (Grant Numbers JP23K14429 and JP22K20734 to MY) and the YOKOYAMA Foundation for Clinical Pharmacology (Grant Number YRY-2207 to MY).

Author contributions

TN carried out the analysis and wrote the manuscript. MY helped with the analysis and revised the manuscript. ST substantially revised the manuscript.

Competing Interests

The authors declare no competing interests.

Data availability

All the codes and results used or generated in the current study are available at our GitHub repository (https://github.com/nakayama-takahiro/i-atac).

Ethics declaration

This study did not generate any original data from animal experiments and human subjects and only analyzed the publicly available datasets from a previous publication (10).

Supplementary Information

The Supplementary File contains Supplementary Figures S1-S3 and their legends.

Figure1

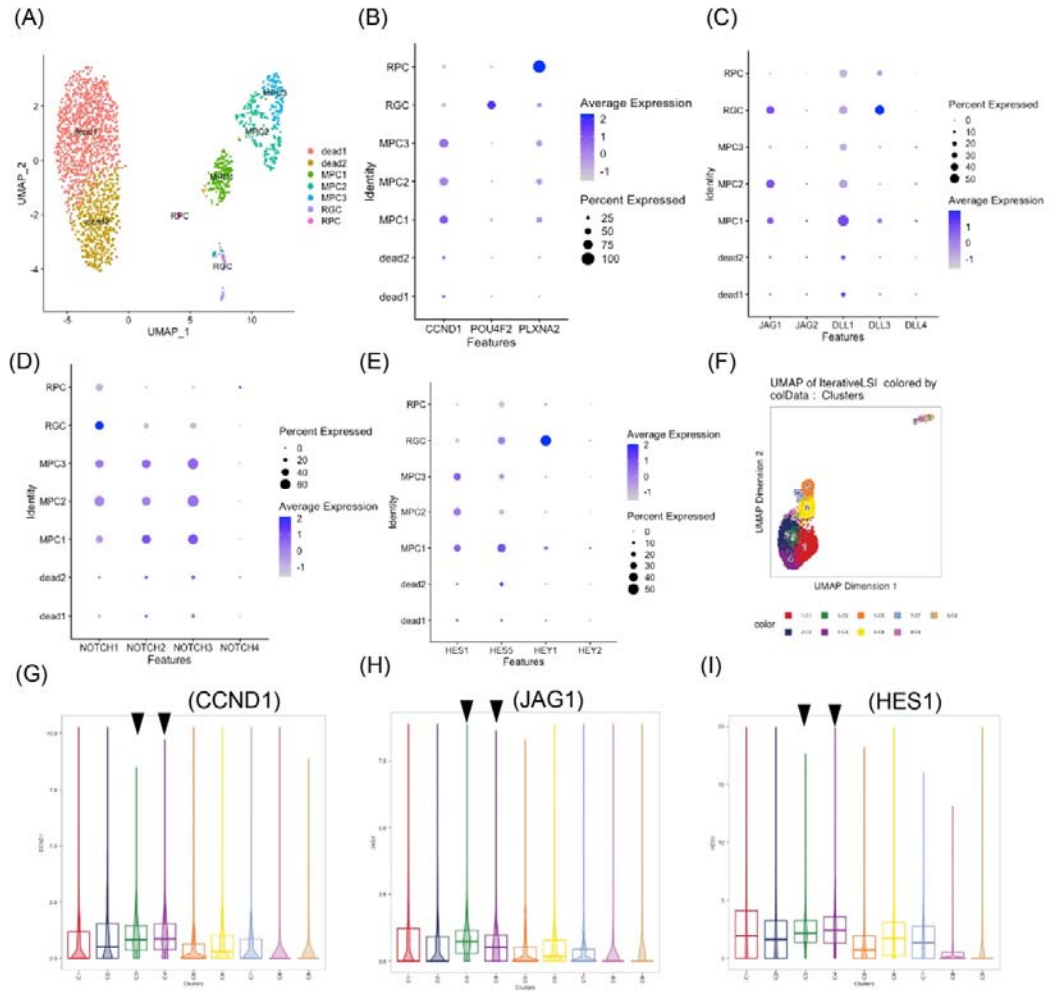

Figure 1 scRNA-seq and scATAC-seq of d53 retinas

(A) UMAP clustering of scRNA-seq data generated seven clusters. (B) Characterization of each cluster with marker genes: CCND1 for MPCs, POU4F2 for RGCs, and PLXNA2 for RPCs. (C) DSL ligand expression in each cluster. (D) NOTCH receptor expression in each cluster. (E) The downstream target gene expression levels in each cluster. (F) UMAP clustering of scATACseq data generated nine clusters. (G) Violin plot of the gene score (chromatin accessibility) for CCND1. Note that the two clusters (C3 and C4; arrowheads) had high scores. (H) Violin plot of the gene score for JAG1. Note the difference between Clusters C3 and C4. (G) Violin plot of the gene score for HES1.

Figure 2

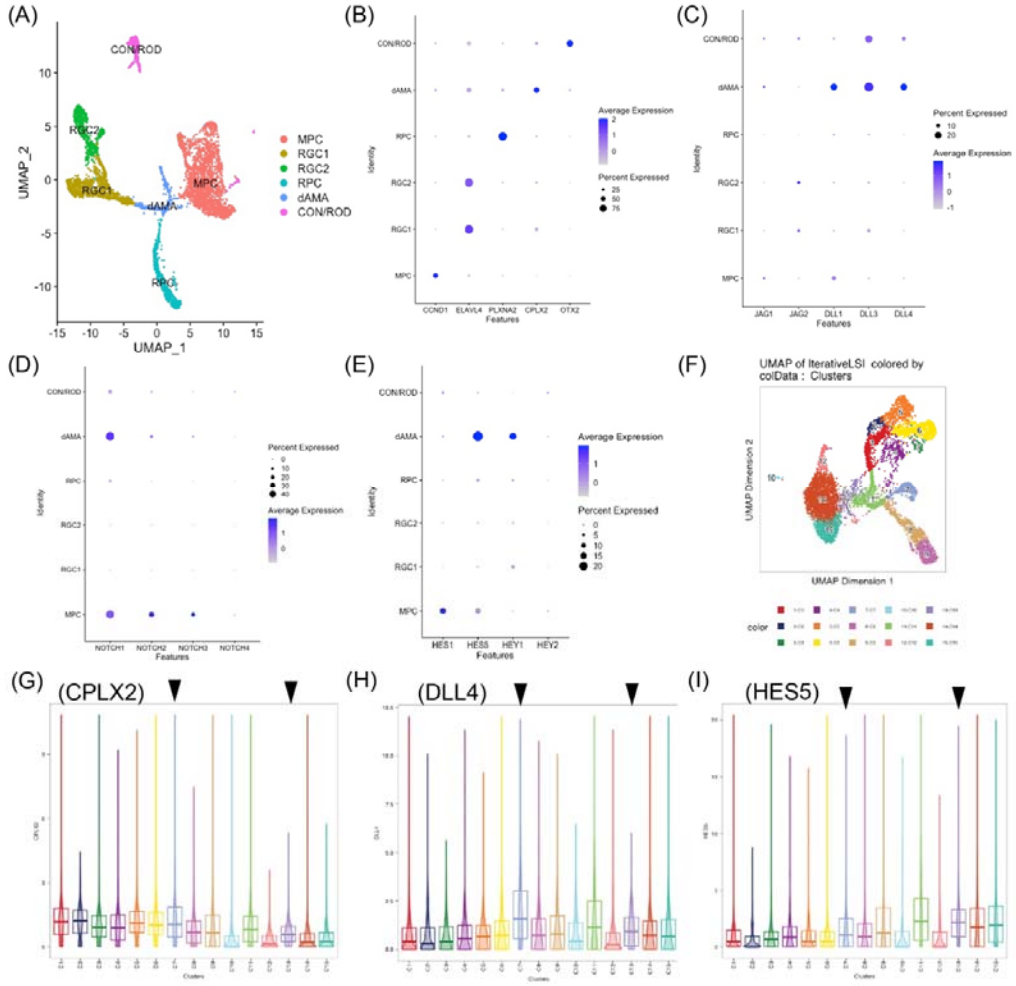

Figure 2 scRNA-seq and scATAC-seq of d59 retinas

(A) UMAP clustering of scRNA-seq data generated six clusters. (B) Characterization of each cluster with marker genes: CCND1 for MPCs, ELAVL4 for RGCs, PLXNA2 for RPCs, CPLX2 for dAMAs, and OTX2 for CON/ROD. (C) DSL ligand expression in each cluster. (D) NOTCH receptor expression in each cluster. (E) The downstream target gene expression levels in each cluster. (F) UMAP clustering of scATAC-seq data generated fifteen clusters. (G) Violin plot of the gene score for CPLX2. C7 and C13 were highlighted with arrowheads. (H) Violin plot of the gene score for DLL4. C7 and C13 were highlighted with arrowheads. (G) Violin plot of the gene score for HES5. C7 and C13 were highlighted with arrowheads.

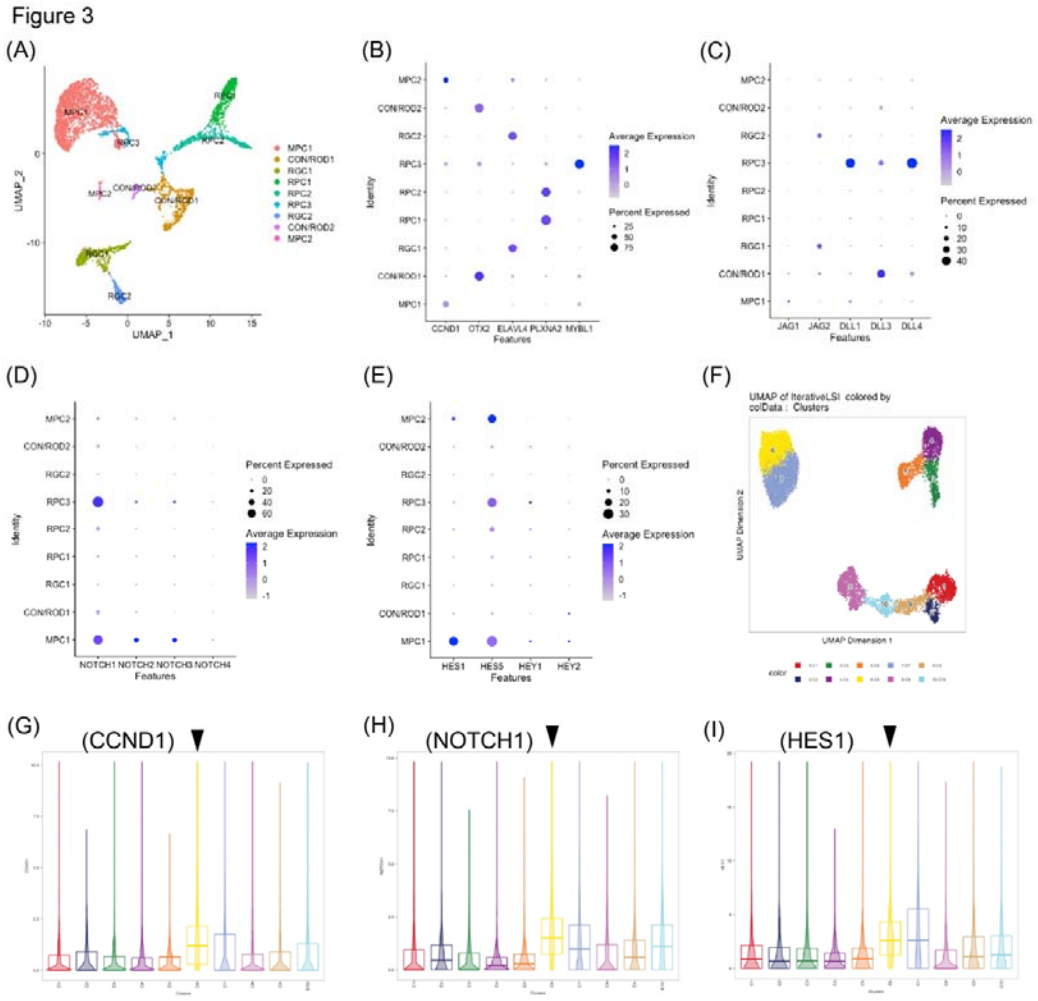

Figure 3 scRNA-seq and scATAC-seq of d78 retinas

(A) UMAP clustering of scRNA-seq data generated nine clusters. (B) Characterization of each cluster with marker genes: CCND1 for MPCs; OTX2 for CON/ROD; ELAVL4, PLXNA2 and MYBL1 for RGCs. (C) DSL ligand expression in each cluster. (D) NOTCH receptor expression in each cluster. (E) The downstream target gene expression levels in each cluster. (F) UMAP clustering of scATACseq data generated ten clusters. (G) Violin plot of the gene score for CCND1. Cluster 6 is highlighted with arrowheads. (H) Violin plot of the gene score for NOTCH1. (G) Violin plot of the gene score for HES1.

Figure1

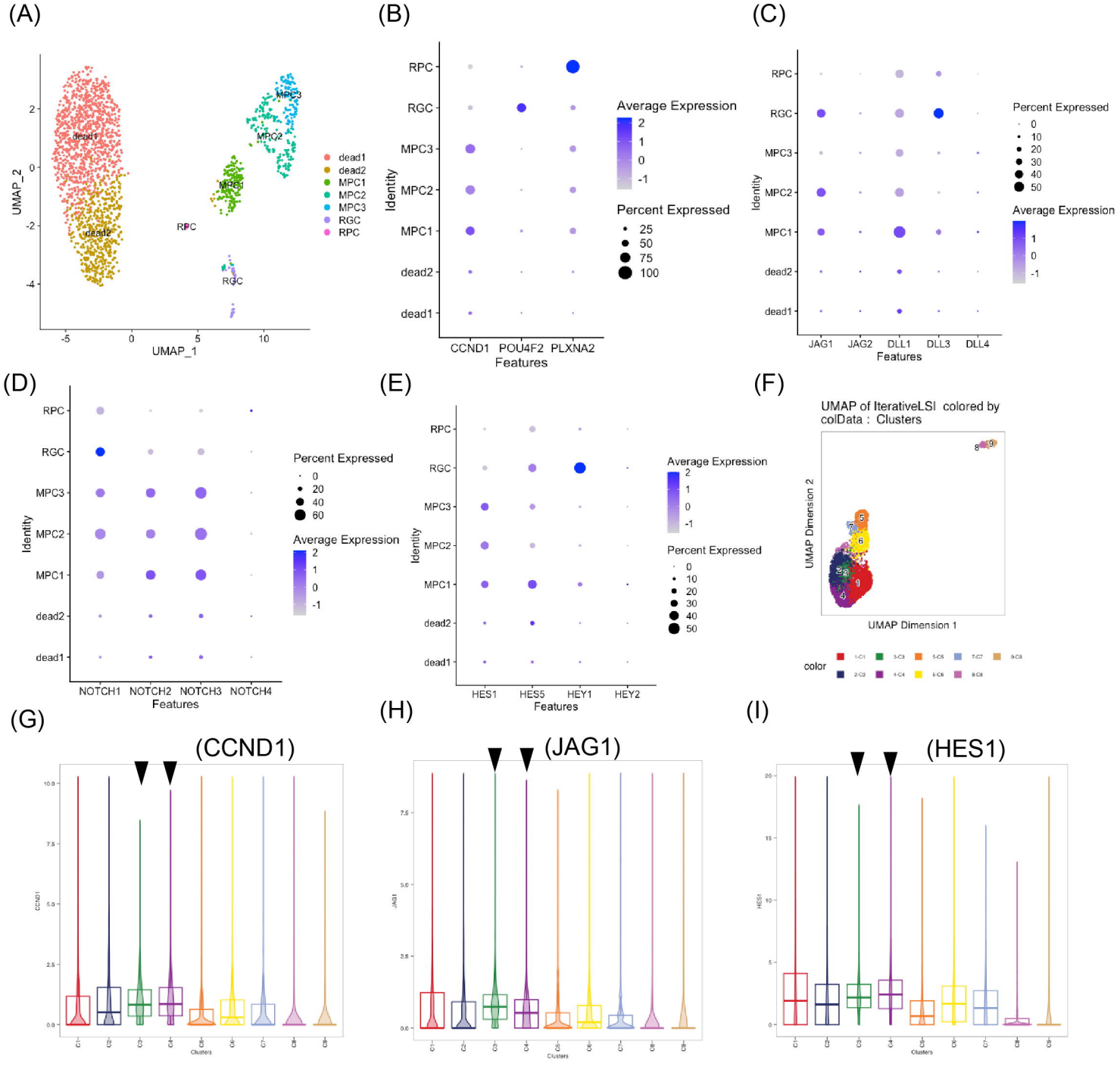
(A)
UMAP_2
UMAP_1
dead1
dead2
MPC1
MPC2
MPC3
RPC
RGC
(B)
Identity
Features
CCND1
POU4F2
PLXNA2
Average Expression
Percent Expressed
(C)
JAG1
JAG2
DLL1
DLL3
DLL4
(D)
NOTCH1
NOTCH2
NOTCH3
NOTCH4
(E)
HES1
HES5
HEY1
HEY2
(F)
UMAP of IterativeLSI colored by colData : Clusters
UMAP Dimension 1
UMAP Dimension 2
color
(G)
(CCND1)
(H)
(JAG1)
(I)
(HES1)

Figure 2

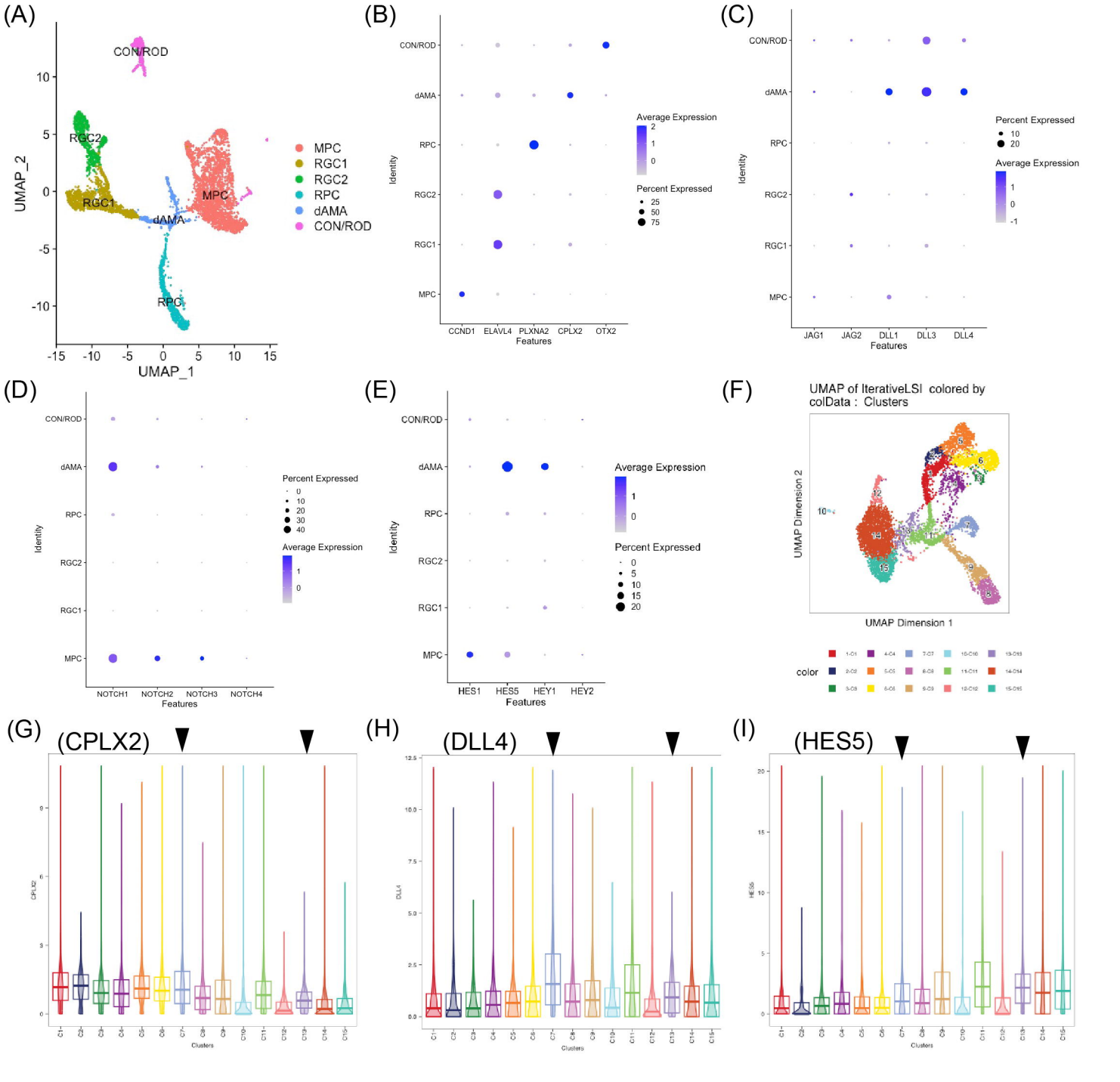
(A)
CON/ROD
RGC2
RGC1
MPC
dAMA
RPC
UMAP_2
UMAP_1
MPC
RGC1
RGC2
RPC
dAMA
CON/ROD
(B)
CON/ROD
dAMA
RPC
RGC2
RGC1
MPC
Identity
CCND1
ELAVL4
PLXNA2
CPLX2
OTX2
Features
Average Expression
Percent Expressed
(C)
CON/ROD
dAMA
RPC
RGC2
RGC1
MPC
Identity
JAG1
JAG2
DLL1
DLL3
DLL4
Features
Percent Expressed
Average Expression
(D)
CON/ROD
dAMA
RPC
RGC2
RGC1
MPC
Identity
NOTCH1
NOTCH2
NOTCH3
NOTCH4
Features
Percent Expressed
Average Expression
(E)
CON/ROD
dAMA
RPC
RGC2
RGC1
MPC
Identity
HES1
HES5
HEY1
HEY2
Features
Average Expression
Percent Expressed
(F)
UMAP of IterativeLSI colored by colData : Clusters
UMAP Dimension 2
UMAP Dimension 1
color
(G)
(CPLX2)
Clusters
(H)
(DLL4)
Clusters
(I)
(HES5)
Clusters

Figure 3

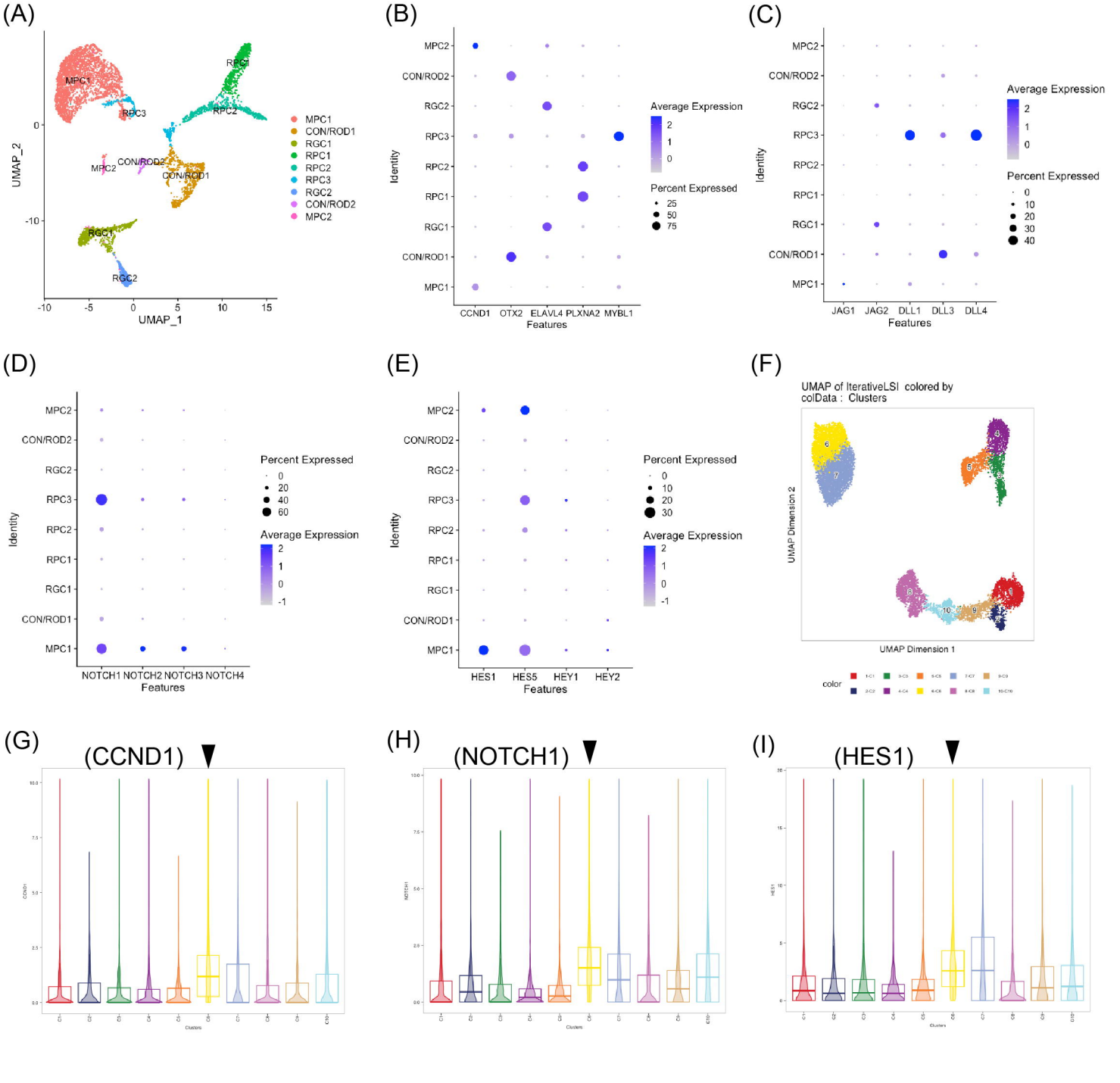
(A)
MPC1
RPC1
RPC3
RPC2
MPC2
CON/ROD2
CON/ROD1
RGC1
RGC2
UMAP_2
UMAP_1
MPC1
CON/ROD1
RGC1
RPC1
RPC2
RPC3
RGC2
CON/ROD2
MPC2
(B)
Identity
Features
CCND1 OTX2 ELAVL4 PLXNA2 MYBL1
Average Expression
Percent Expressed
(C)
Identity
Features
JAG1 JAG2 DLL1 DLL3 DLL4
Average Expression
Percent Expressed
(D)
Identity
Features
NOTCH1 NOTCH2 NOTCH3 NOTCH4
Percent Expressed
Average Expression
(E)
Identity
Features
HES1 HES5 HEY1 HEY2
Percent Expressed
Average Expression
(F)
UMAP of IterativeLSI colored by colData : Clusters
UMAP Dimension 1
UMAP Dimension 2
color
(G)
(CCND1)
(H)
(NOTCH1)
(I)
(HES1)